Strong surface-pinning effects in polycrystalline $HgBa_2CuO_{4+\delta}$ superconductors

Yang Ren Sun
Department of Physics, The University of Tennessee, Knoxville, Knoxville, Tennessee 37996-1200

J. R. Thompson
Department of Physics, The University of Tennessee, Knoxville, Knoxville, Tennessee 37996-1200
and Solid State Division, Oak Ridge National Laboratory, P.O. Box 2008, Oak Ridge, Tennessee 37831-6061

H. R. Kerchner and D. K. Christen
Solid State Division, Oak Ridge National Laboratory, P.O. Box 2008, Oak Ridge, Tennessee 37831-6061

M. Paranthaman and J. Brynestad
Chemical and Analytical Sciences Division, Oak Ridge National Laboratory, P.O. Box 2008, Oak Ridge, Tennessee 37831-6100
(Received 3 March 1994)

Magnetic studies on polycrystalline $HgCa_2CuO_{4+\delta}$ superconductors reveal pronounced pinning by the grain surfaces at low temperatures over a wide range of magnetic fields. The response to small ac fields shows that up to 80% of the width of the dc magnetic hysteresis loop in high fields originates from shielding supercurrent flowing in the surface sheath, a vortex-free region with thickness of ~ 10 nm. At 10 K and 15 kG, the observed persistent surface current has a density of $\sim 5\times 10^7$ A/cm^2 when averaged over the barrier thickness. The study suggests that a high current density may be achieved in very thin films by surface pinning.

INTRODUCTION

The recent discovery of a new family of superconducting materials, the mercury-based copper oxides,[1] has further stimulated interest and enthusiasm in high temperature superconductors. Preliminary studies have revealed many aspects of these novel materials.[2,3] A particularly pronounced feature is that they have high transition temperatures T_c, similar to the thallium- and bismuth-based materials, whose value increases with the number of copper-oxide sheets. New records of 134 K (at ambient pressure)[4] and 164 K (under hydrostatic pressure)[5] were established for the $HgBa_2Ca_2Cu_3O_{8+\delta}$ (Hg-1223) compound. In addition, higher irreversibility lines for the materials are very attractive.[6] In this work, we report the study of another unique feature observed on a Hg-1201 polycrystal sample, the effect of significant surface pinning at low temperatures over a wide range of magnetic fields.

It is well known[7,8] that an ideal surface of a type-II superconductor provides an intrinsic pinning barrier, the Bean-Livingston (BL) barrier, which impedes entry or exit of vortices. The phenomenon arises from a competition of two effects: (1) an attraction toward the surface for an entering flux line, due to its image line that is mirrored by the material boundary, and (2) a repulsion from the surface, due to the interaction of the flux line with induced supercurrents. The net result is that, when $H < H_p$, vortex lines cannot penetrate into the sample; here the penetration field is $H_p \approx \kappa H_{c1} \approx H_c$, the Ginzburg-Landau parameter is $\kappa = \lambda/\xi$ (λ is the penetration depth and ξ is the coherence length), H_{c1} is the lower critical field, and H_c is the thermodynamic critical field. In practice, surface effects in low-temperature superconductors can be neglected in most cases due to relatively strong bulk pinning and especially to imperfections in the specimen surface. For high-temperature superconductors, Burlachkov *et al.*[9] pointed out that even if the effect is suppressed due to surface roughness, the large values of H_c lead to higher values for H_p, making the BL barrier very pronounced. In studies on $YBa_2Cu_3O_7$ (Refs. 9 and 10) and $Bi_2Sr_2CaCu_2O_8$ (Ref. 11) crystals, pronounced surface pinning effects have been observed. However, the presence of strong bulk pinning at low temperatures means that most experiments are performed at temperatures either near to T_c as in $YBa_2Cu_3O_{7-\delta}$, or close to the irreversibility line (BSCCO). In either case, the magnetic-field range is relatively small. Recent work on $YBa_2Cu_4O_8$ crystals has shown the presence of distinct surface barrier effects in magnetic fields up to 1 T, followed by a sudden onset of bulk pinning at higher fields.[12]

In this work, we observe strong surface effects in randomly oriented $HgBa_2CuO_{4+\delta}$ (Hg-1201) polycrystalline materials at low temperatures for a wide range of magnetic fields. These effects are associated with the surfaces of individual grains that are mostly decoupled. The physics deals primarily with intragranular effects, while intergrain current conduction constitutes a perturbation that will be subtracted out. The first piece of evidence for strong surface effects is that the magnetic hysteresis loops are very asymmetric with respect to increasing versus decreasing field branches. In contrast, the normal situation, where bulk pinning dominates, gives symmetric loops.

0163-1829/94/50(5)/3330(7)/$06.00

The characteristic flat magnetization curve for the field decreasing branch with values close to zero is clearly seen. The second piece of evidence is that the flux-creep rate, $dM/d\ln(t)$, at fixed temperatures and fields is magnetically asymmetric; with increasing field history, it is about twice as large as with decreasing field history. The third and conclusive piece of evidence is the magnetic response to small ac fields. Comparing the ac moment as a function of ac field amplitude with calculations based on the theory of Clem[13] and Burlachkov[14] shows that the width of the hysteresis loop comes mainly from surface currents. The density of the surface current is as large as 5×10^7 A/cm^2 at $T=10$ K and $H=15$ kG.

EXPERIMENTAL ASPECTS

A randomly oriented $HgBa_2CuO_{4+\delta}$ polycrystal was used in these studies. Details of the sample preparation have been reported elsewhere.[15] X-ray diffraction showed that the sample was single phase with lattice parameters of 3.876 Å (a axis) and 9.515 Å (c axis). The sample was cylindrical with diameter of 3.2 mm, length of 5.8 mm, and mass of 253 mg. The corresponding apparent density of the specimen was 76% of the theoretical density (7.05 g/cm^3), as calculated from the crystal lattice constants. The typical grain size of the individual particles was approximately 3 μm, as determined by transmission electron microscopy (TEM).

The dc magnetic measurements were made by using a commercial SQUID magnetometer (Quantum Design MPMS-7) and a laboratory-constructed vibrating sample magnetometer (VSM). The superconducting quantum interference device (SQUID) magnetometer is equipped with a 7-T magnet which can maintain the sample in a highly homogeneous field during measurement scans. The VSM has an additional advantage that it allows for continuous observation of the magnetic hysteresis curves on an x-y recorder, which is particularly useful for studying the reaction when one changes the direction of the field scan.

The ac studies were conducted using a laboratory-built mutual inductance bridge (MIB). A small ac field was applied coaxially with a dc field for study of the magnetic response to the applied total field $H_{ap}=H_{dc}+h_0\sin(\omega t)$. The ac field induces a signal in a set of pickup coils that is proportional to the time derivative of the ac moment m_{ac} of the specimen. A two-phase lock-in amplifier (PAR model 5210) used without preamplifier filtering integrated the voltage over half cycles and provided the magnetic-moment change over a half cycle of the applied sinusoidal field. A standard resistor in series with the ac primary coil generated a reference signal and established the phase for the phase sensitive detector. Two rectified, dc-output voltages V_{ind} and V_{res}, respectively proportional to the real and imaginary parts of m_{ac}, were produced. All magnetic measurements were performed with field parallel to the cylinder axis. For uniform and consistent calibration of the several instruments, a high-quality, homogeneous Nb superconducting sphere was used as a standard magnetic moment.

dc RESULTS AND ANALYSIS

Figure 1 presents the dc susceptibility $\chi=M/H_{eff}$ as a function of temperature, for small magnetic fields of 4 and 25 G. Here (and only here), we calculated the magnetization using the "geometrical volume" as determined from the sample dimensions, in order to account properly for screening effects. As noted above, due to sample porosity, this volume was about 24% larger than that calculated from the mass and x-ray density. The effective demagnetization factor D, calculated from the length-to-diameter ratio of the cylindrical sample,[16] was 0.20 and this was used to calculate the effective magnetic field H_{eff}. As seen in the figure, the quantity $4\pi\chi$ is almost equal to -1. This means that at low temperatures the sample interior was completely shielded by intergranular supercurrents. For the most part, these currents flow through weakly coupled boundaries. With increasing temperature, the coupling between grains deteriorated, allowing magnetic flux to thread between the grains at their boundaries. The entry of the flux corresponds to the "knees" in the zero-field-cooled (ZFC) curves in Fig. 1. For low fields, the knee lies near T_c; e.g., with $H=4$ G, it is barely visible at $T=93$ K. With higher fields, however, the intergrain Josephson current conduction deteriorates at much lower temperatures; thus the knee is clearly visible near $T=78$ K for $H=25$ G. Further evidence supporting this interpretation was discussed earlier.[15] Another feature of this sample is a strong flux expulsion (Meissner effect) by the individual grains, as shown by the field-cooled (FC) curve with $H=25$ G. To illustrate this point, we have drawn a horizontal dotted line to smoothly connect with the knee in the corresponding ZFC curve ($H=25$ G). This line represents the ZFC curve (shielding signal) for an average individual grain that would have been observed, *if* the grains were thoroughly decoupled. By comparing the FC curve with the simulated (dotted) ZFC line, we see that up to 75% of the ZFC intragrain flux was expelled. This indicates that the individual grains were relatively homogeneous with weak pinning within the grains.

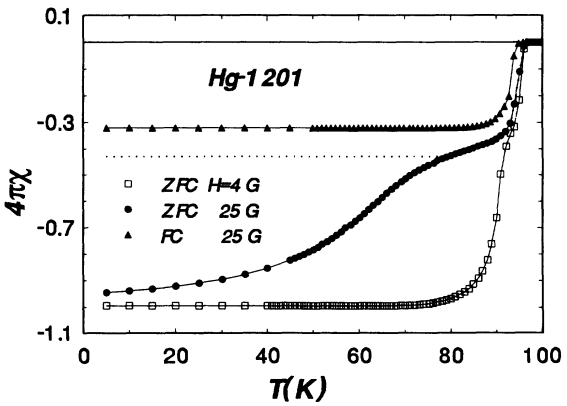

FIG. 1. The dc susceptibility $4\pi M/H_{eff}$ versus temperature T for polycrystalline $HgBa_2CuO_{4+\delta}$, for applied magnetic fields of 4 and 25 G. The dotted line visualizes the zero-field-cooled (ZFC) response in 25 G, if the grains were fully decoupled.

Magnetic hysteresis loops $M(H;T)$ at $T=5$ and 15 K are presented in Fig. 2. A striking feature is the very asymmetric shape of the curves, when one compares the field increasing versus field decreasing branches. This asymmetry conflicts with the Bean model, which provides for a magnetic hysteresis loop that is symmetric about the $M=0$ axis (neglecting contributions from the equilibrium magnetization). Furthermore, the magnetization in the field decreasing branch is very small, suggesting[13,14] that surface pinning dominates in the material. Note that these features extend up to at least 65 kG, an enormous range of field. Magnetization measurements at other temperatures were similar and showed that the loop width diminished quickly with increasing temperature. While similar observations on $YBa_2Cu_3O_{7-\delta}$ single crystals[9,17] and $Bi_2Sr_2Ca_1Cu_2O_8$ crystals[11] have been reported, the temperatures were generally much higher. Indeed, it is highly unusual to observe strong surface effects at low temperatures over a wide range of fields, as demonstrated in this work.

To further characterize this system, magnetic relaxation measurements were conducted at fixed temperatures using a VSM. For flux entry into the material, the field was swept directly from zero to the target value, after which the flux creep (M versus time t) was measured. For flux exit, H was swept first to some considerably higher field and then decreased to its target value, always ensuring that the flux front fully penetrated the material. The magnetization $M(t)$ was recorded as a function of time for about 5 min, beginning immediately when the field reached its target value. Figures 3(a) and 3(b) show M versus $\ln(t)$ for flux creeping "out" and "in", respectively. Comparing the two figures, we see clearly that the rate of flux entry is about twice as large as the exit rate, which would not happen for a system with pure bulk pinning.

However, two aspects appear to be inconsistent with theory for surface barrier pinning.[14] One is the field dependence of the entry magnetization, $M_{en}(H)$. Above the field of first penetration H_p, the following relation is expected:

$$-4\pi M_{en}=H-\sqrt{H^2-H_p^2}\approx H_p^2/(2H)\ . \qquad (1)$$

To test this dependence, Fig. 4 shows VSM results for

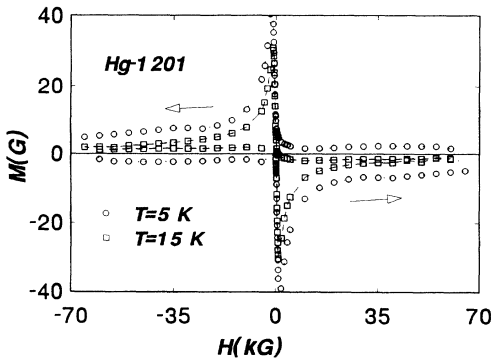

FIG. 2. Magnetization loops $M(H)$, measured at 5 and 15 K.

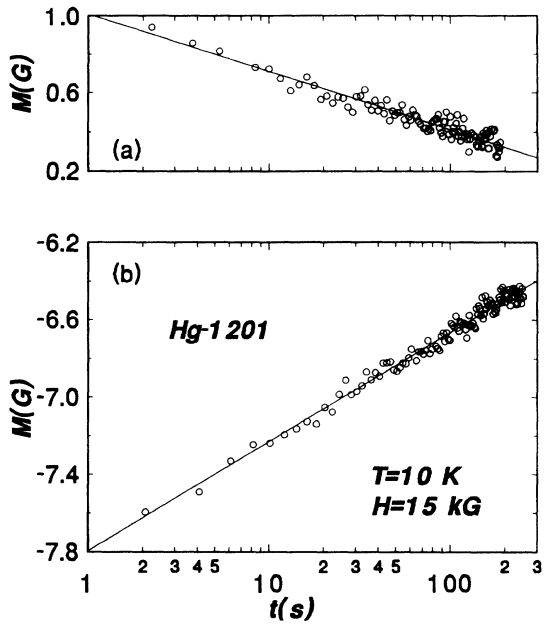

FIG. 3. Time dependence of the magnetization M at 15 kG and 10 K, versus time on a log scale. (a) Results for decreasing field history and (b) increasing field history, respectively. The vertical scale factors are identical.

$M(H)$ at $T=10$ K. [The VSM has the advantage that it continuously measures $M(H)$ and so determines H_p better.] As seen in the figure, the magnetization decreases too slowly to fit the inverse field dependence $M\propto 1/H$. A second apparent inconsistency is the ratio between rates of flux entry and exit, R_{en}/R_{ex}. This ratio is smaller than the value predicted by the theory:[14]

$$R_{en}/R_{ex}=3(M_{en}/M_{eq})^{3/2}\approx 3\kappa^{3/2}(H_p/H)^{3/2}\ . \qquad (2)$$

Here $R=dM/d\ln(t)$ and M_{eq} is equilibrium magnetiza-

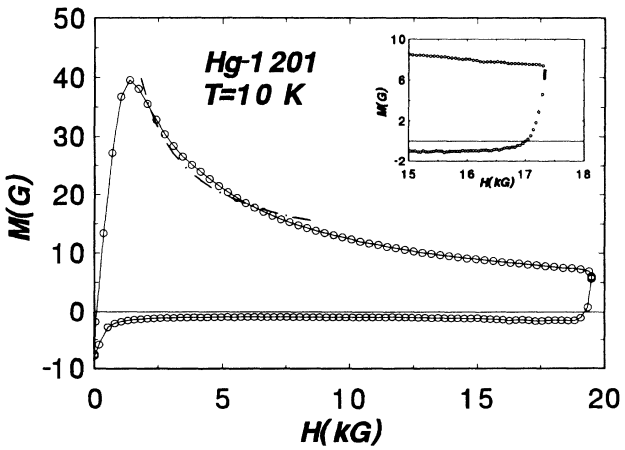

FIG. 4. A magnetization loop $M(H)$ at 10 K, measured by VSM. The dashed line on the upper branch represents the inverse relation $M\propto 1/H$ predicted by surface pinning theory for uniaxial materials. Inset: detailed response of $M(H)$ upon changing the direction of field scan. Here the field was swept at 4 G/s.

tion. To evaluate this expression, we use experimental results[18] from an analysis based on vortex fluctuation theory,[19,20] which provided the values $\lambda_{ab}(0)=0.12\ \mu$m, $\xi_{ab}(0)=2.1$ nm, and $\kappa=45$ for this compound. Substituting $H_p=1200$ G and $H=15\,000$ G into Eq. (2), we obtain $R_{en}/R_{ex}=20$, which is substantially higher than the experimental result.

One possible origin for these inconsistencies is that the theory treats an isotropic or uniaxial system with unique values of H_p and κ. In contrast, the material here is a randomly oriented polycrystal. Hence the value of H_p for each grain may vary, depending on its orientation. Thus, it is not appropriate to use a single value of H_p to fit the magnetization curve. The same consideration applies to the analysis of R_{en}/R_{ex}, where a distribution of κ and H_p should be taken into account. Alternatively, if we substitute in Eq. (2) the experimental value ~ 7 G for M_{en} and ~ 3.3 G for M_{eq} (as calculated using vortex fluctuation theory with parameter values from Ref. 18), then the ratio is about 9. This is closer to the experimental result, but still larger.

To confirm further that the observed phenomena arise from surface-pinning effects, we studied the ac response. As discussed below, a sample's response to a small ac field provides a very useful way to distinguish surface pinning from bulk pinning. In addition, it gives quantitatively the contribution of surface pinning to the overall magnetization, the scale of the surface sheath, and the surface supercurrent density.

ac RESPONSE

According to the BL theory,[7] an *ideal* surface of a type-II superconductor permits entry of an applied external field not at H_{c1}, but rather at some higher field $H_p \approx H_c$. For surfaces that are *nonideal* due to microscopic imperfections and/or angular misalignment, one expects penetration at some field below the ideal H_p. The surface barrier, which arises from the competition of forces previously discussed, leads to a vortex-free region near the surface.[13,21] For a cylindrical sample of radius $R \gg \lambda$ in which bulk pinning is negligible, the magnetic flux density B inside the material can be considered uniform. In this case, the thickness of the vortex-free region x_f is determined by the relation

$$x_f=\lambda \cosh^{-1}(H/B)\ . \tag{3}$$

The local magnetic field H within the vortex-free region decreases from its surface value $h(r=R)=H$ to its interior value B over the distance x_f, as described by the equation:

$$h(x)=B\cosh[(x_f+x-R)/\lambda]\ . \tag{4}$$

We assume that at some time $t<0$, an dc external field $H_0>H_p$ was applied; these static conditions give the values B_0 for the vortex flux density and x_{f0} for the annular thickness. At $t>0$, a small ac field $h_{ac}(t)\ll H_0$ is added parallel to the dc field. Both B and x_f will oscillate in reaction to the ac field. Let us consider the case with $h_{ac}\ll 4\pi M_{en}$, where M_{en} is the magnetization when the surface barrier to flux entry is zero, as illustrated in Fig. 1 of Ref. 13. The effects of magnetic relaxation on the ac response are small,[13,14] because a large quasistatic surface barrier prevents cyclic entry and exit of flux. For simplicity, then, we neglect flux-creep effects in the following discussion. Hence, the number of vortices is conserved and the equations for $x_f(t)$ and $B(t)$ are the following:

$$\pi B(t)(R-x_f)^2=\pi B_0(R-x_{f0})^2\equiv\Phi\ , \tag{5}$$

$$2[(H/B)-1]=(x_f/\lambda)^2\ , \tag{6}$$

where $H(t)=H_0+h_{ac}(t)$. We obtain Eq. (6) from Eq. (3), assuming $x_f/\lambda\ll 1$. Combining Eqs. (5) and (6) gives the following for B:

$$B^2\left[1+2\frac{\lambda^2}{R^2}\right]^2+B\left[\frac{4\Phi\lambda^2}{\pi R^4}-\frac{2\Phi}{\pi R^2}-\frac{8H\lambda^4}{R^4}-\frac{4H\lambda^2}{R^2}\right]+\left[\frac{\Phi}{\pi R^2}-\frac{2H\lambda^2}{R^2}\right]^2=0\ . \tag{7}$$

The magnetic flux in the vortex-free region is calculated by integrating $h(r)$ from Eq. (4) as follows:

$$\phi=2\pi\int_{R-x_f}^{R_f}h(r)r\,dr$$
$$=2\pi\lambda B\left[R\sinh\left[\frac{x_f}{\lambda}\right]+\lambda\left[1-\frac{H}{B}\right]\right]\ . \tag{8}$$

The ac moment m_{ac} is directly related to the net time-dependent flux $[\pi R^2 h_{ac}-(\phi+\Phi)]$. Consequently, comparing the ac experiments with these calculations can provide several interesting quantities, including the surface related magnetization, x_f, and B_0.

As mentioned earlier, the ac magnetometer detects both the real and imaginary phases of m_{ac}. Instrumentally, the phase sensitive detector generates the real (inductive) component M_{ind} by integrating the ac voltage from $\omega t=-\pi/2$ to $\omega t=\pi/2$ and subtracting the voltage integrated from $\pi/2$ to $3\pi/2$; the imaginary part m_{res} comes from integrating from $\omega t=0$ to $\omega t=\pi$ and subtracting the integral from π to 2π. This provides the key results shown in Fig. 5, where the components of ac magnetization M_{res} and M_{ind} are plotted as functions of ac amplitude h_0, respectively. The open symbols in the figure denote the raw experimental measurements. These representative data were taken at $T=10$ K and $H_0=15$ kG.

Below, we show that surface effects account very well for the results in Fig. 5. First, however, we eliminate relatively unimportant influences of intergranular currents; then we rule out explanations based on bulk intragranular pinning; and finally we compare our experimental results with the theoretical analysis cited.

Examination of Fig. 5 shows that two sources contribute to the magnetization M_{ind}, as evidenced by its abrupt change of slope near $h_0\approx 7$ G. For convenience, we denote the regions as segment 1 for $h_0<7$ G and segment 2 for $h_0>7$G, respectively. In segment 1, the differential susceptibility $\chi=dM_{ind}/dh_0$, is unphysically large, with

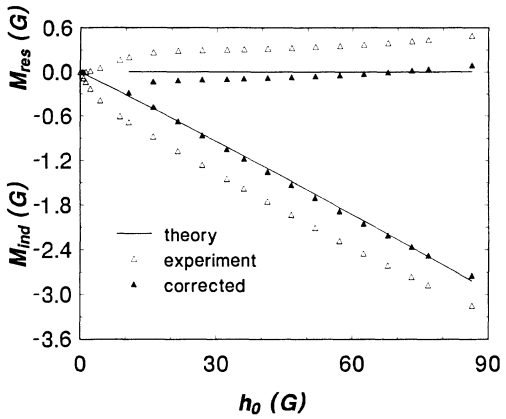

FIG. 5. The ac magnetization versus ac field amplitude h_0, for the out-of-phase component M_{res} and the in-phase component M_{ind}. The solid lines show calculated in-phase ac magnetization M_{theor} and out-of-phase component. Raw experimental values (open symbols) were corrected (filled symbols) in the region with $h_0 > 10$ G, by subtracting the contribution (-0.4 G) due to intergranular currents.

$4\pi\chi = -1.204$ for $h_0 \to 0$. This value is based on the mass volume, i.e., (mass-theoretical density), with no correction for demagnetizing effects. Using the geometrical volume gives $4\pi\chi = -0.803$. In either case, these large values clearly indicate that a weak *ac intergranular* current circulates through a portion of the material, even with a dc field $H_0 = 15$ kG. (This observation does not conflict with the lower field dc results in Fig. 1, which show that *most* of the grains are weakly linked on the long time scale of the dc experiment.) As a result of some grain-to-grain coupling, a small ac field can induce intergranular currents. However, the current is limited by the very small fraction of strongly linked grains, which causes this contribution to M_{ind} to saturate with a value of -0.4 G near $h_0 = 7$ G. In region 2, we subtract out this intergrain contribution (-0.4 G) to obtain the grain-surface-related, majority component of M_{ind}, which is denoted by filled symbols.

Considering the out-of-phase magnetization M_{res}, Fig. 5 shows that there is little loss for small ac fields, but the loss increases quickly when h_0 exceeds 1 G and flattens for $h_0 > 14$ G. This behavior is attributed to the same intergrain currents, which are easily driven to their critical values. Consequently, an intergrain loss component develops and saturates in concert with the development and saturation of the inductive component. Now, for a superconducting current ring driven to its critical current, the real and imaginary components of M are equal in magnitude. They differ mainly in that the ac field amplitude h_0 needed for saturation of M_{res} must be twice as large[22] as that required for M_{ind}. Consequently, we make the same 0.4 G correction for M_{res} as for M_{ind}, except that h_0 must be $> \sim 14$ G. The corrected values are shown as filled symbols in Fig. 5.

Let us now establish that the results in Fig. 5 cannot be explained by bulk pinning of vortices. Campbell[23] has shown, for example, that in a bulk pinning system, (1) the in-phase flux is proportional to the square of the ac amplitude and furthermore, (2) the in-phase flux is twice the out-of-phase flux. Experimentally, however, the in-phase flux $\pi R^2(h_{ac} + 4\pi M_{ind})$ has no h_0^2 dependence in either segment 1 or 2. Furthermore, the value of M_{ind} is much larger than its corresponding value of $2M_{res}$. These discrepancies persist, independent of the above treatment of intergranular effects. Hence it is clear that ordinary bulk pinning is not significant in the materials under study. Rather, surface effects dominate the magnetic behavior.

The most interesting data in Fig. 5 is contained in segment 2. For h_0 in the range 10–70 G, M_{ind} increases linearly with ac amplitude, with slope $dM/dh_0 = -0.032$. Meanwhile, the corrected M_{res} is very nearly zero, rising slowly with ac field amplitude. Both major features are quantitatively consistent with the presence of a surface barrier, as shown below. For amplitudes above ~ 70 G, the slope of M_{ind} gradually decreases, while M_{res} rises more quickly.

It is interesting to compare and combine these measurements with the dc results in Fig. 4. The dc hysteresis loop in the main figure was acquired with a field sweep rate $dH/dt = 160$ G/s. The figure shows that at $H = 15$ kG, M_{en} is about -8.2 G and M_{ex} is 1.1 G. The positive value of M_{ex}, which is ideally zero, can arise from intergranular shielding currents and perhaps a minor amount of bulk pinning. The inset (Fig. 4) shows the hysteresis loop for dc fields in the range 15 kG $< H <$ 17.3 kG, taken at a sweep rate of 4 G/s for higher resolution. The response of the system to changing the direction of field scan is easy to see. When the scan with increasing field was stopped at 17.3 kG for a few seconds, the signal decayed due to flux creep, generating the vertically aligned points. Upon sweeping the field downward, the magnetization decreased *linearly* with H to a value of ~ -0.2 G, and then approached M_{ex} more gradually. The linear variation, indicated by a dotted line, has a slope of -0.032. It is almost the same slope as that found in segment 2 of the ac data, Fig. 5. This agreement strongly suggests that the underlying mechanism governing the response of the magnetization is the same in the ac and dc studies.

We now analyze m_{ac} with Eqs. (7) and (8), using the following material parameters. From TEM micrographs, an average grain diameter of ~ 3 μm was obtained. For the London penetration depth, we have $\lambda_{ab}(0) = 0.117$ μm from an analysis of vortex fluctuation effects.[18] The value of Φ [see Eq. (5)] depends on the value of the approximately constant internal induction B_0. If bulk pinning and the thickness of the vortex-free region are neglected, then the relation $B_0 \approx H_0 + 4\pi M_{en}$ provides a good estimate of B_0. Taking $M_{en} = -8$ G from Fig. 4 and $H_0 = 15\,000$ G, one obtains $B_0 - 14\,900$ G. The value of $x_{f0} = 10$ nm is then obtained from Eq. (3).

The calculated results for m_{ac} (solid lines) are plotted versus h_0 in Fig. 5 for comparison with the experimental data for M_{ind}. A key feature is that in the region $h_0 > 10$ G, the calculated lines lies highly parallel to the raw data. After correction for intergranular currents, the experi-

mental results (shown as solid symbols) agree quite well with the calculated curve. Furthermore, the lossy component M_{res}, as corrected, is quite small; this is just what one expects for a system with surface barriers, where the ac field compresses and expands the vortex array *very* slightly during each cycle. These features give strong evidence that surface barrier effects dominate in these materials and constitutes a central result of this work.

For still higher ac field amplitudes ($h > 70$ G in Fig. 5), the experimental measurements curve upward. We suggest that this diminishing response for M_{ind} comes from the onset of increasingly significant amounts of flux ingress and egress in large h_0. This feature is not included in the above theory, which assumes that flux-creep effects are negligible. Also, the increase of the lossy component M_{res} at high h_0 may affect the inductive component as well, since the model does not include any loss which becomes important for large ac amplitudes. Hence the increase of the loss signal reduces the in-phase signal and the magnitude of M_{ind}.

At sufficiently high amplitude of the ac field, one expects the barrier-related ac moment to saturate. Unfortunately, the maximum available ac field was ~90 G, due to limitations of the power supply and heating effects in the MIB. We can circumvent this limitation and determine the net contribution to the magnetization from surface currents, by incorporating some results from the dc study into the analysis. As noted before, the *ac* slope dM_{ind}/dh_0 for $h_0 =$ 10–70 G, is nearly the same as the *dc* slope dM/dH_0 in the domain where the field sweep reverses direction. This means that both have the same origin. As shown by the inset in Fig. 4, the magnetization varies linearly with decreasing H, with M changing from -8.2 to ~ -1 G. (While the inset shows data at $H_0 = 17\,000$ G, the corresponding results at $H_0 = 15\,000$ G are very similar.) Hence surface pinning furnishes 7.2 G of the irreversible magnetization. The remaining -1 G of magnetization change in this loop comes from bulk pinning contributions. Combining these results with the calculated thickness ~10 nm of the vortex-free region, one finds for the corresponding surface current density at 10 K and 15 kG a value of 5×10^7 A/cm^2, averaged over the boundary thickness. This is about ($\frac{1}{8}$) of the depairing current density for $H \| c$ axis, as calculated using standard expressions.

Surface barriers appear to be somewhat common in Hg-based high-temperature superconductors. For example, we have obtained similarly asymmetric dc magnetization curves for other Hg-based superconductors, both $HgBa_2CaCu_2O_{6+\delta}$ and $HgBa_2Ca_2Cu_3O_{8+\delta}$. Others[24,25] have presented (without explanation) similar $M(H)$ loops for as-synthesized Hg-1201 materials. So materials produced elsewhere also exhibit clear evidence of surface barrier effects well below T_c in large magnetic fields. Moreover, upon neutron irradiation that increased the bulk pinning, the magnetization loops became much more symmetric about the zero of magnetization.[25] These observations further confirm the validity of our explanation in terms of surface barrier effects.

Observation of pronounced surface barriers requires that a bulk pinning effect be small by comparison. In crystals of high-T_c materials, this has been achieved largely by operating at temperatures and fields above the irreversibility line, where the bulk $J_c \to$ O. However, for the Hg-based materials investigated here, the magnetization studies were conducted well below the irreversibility line, where the intergrain persistent current density was finite but comparatively small. The weakness of current density arise either from low densities of naturally occurring defects (e.g., due to synthesis at unusually low temperatures for the Hg-based compounds), or from less favorable fundamental properties such as a lower thermodynamic critical field H_c and condensation energy, or from a combination of these. Another factor that can promote the observability of surface effects is a large surface-to-volume ratio in the superconducting grains. As noted by Beasley, Labusch, and Webb,[26] the creep rate scales as R^2 for a surface barrier and as R^3 for pure bulk creep. Thus, surface effects are accentuated in very small particles. However, the grain size in the present study, 3 μm, is roughly comparable with those in many other studies of polycrystalline or grain aligned high-T_c superconductors, such as $YBa_2Cu_3O_{7-\delta}$. For these other comparably sized high-T_c particles, bulk rather than surface effects tend to dominate at low temperatures. Qualitatively, we attribute this to a greater density and effectiveness of naturally occurring pinning. In addition, defects at the surface degrade the effectiveness of the surface barrier. In the specific case of $YBa_2Cu_3O_{7-\delta}$, twin boundaries can act as "gates" to channel flux into the interior.[9]

CONCLUSIONS

Pronounced surface-pinning effects have been demonstrated in polycrystalline Hg-1201 materials. Even at low temperatures, surface pinning rather than bulk pinning dominates the magnetic properties of these Hg-based samples. The response of the surface shielding current to a small ac field, superposed on a large dc field, has been discussed in terms of a model based on Clem's theory. In this case, the calculated surface current density is about 5×10^7 A/cm^2 at 10 K of temperature and 15 kG of dc field.

ACKNOWLEDGMENTS

We wish to thank Z. L. Wang, who performed the electron microscopy. The Science Alliance at the University of Tennessee supported a portion of the work of YRS and JRT. The research was sponsored by the Division of Materials Sciences, U.S. Department of Energy, and technology development was funded by the U.S. Department of Energy, Office of Advanced Utilities Concepts-Superconductivity Partnerships Program, both under Contract No. DE-AC05-84OR21400 with Martin Marietta Energy Systems, Inc.

[1]S. N. Putilin, E. V. Antipov, O. Chmaisse, and M. Marezio, Nature (London) **362**, 226 (1993).
[2]D. K. Christen and J. R. Thompson, Nature (London) **364**, 98 (1993).
[3]A. Umezawa, W. Zhang, A. Gurevich, Y. Feng, E. E. Hellstrom, and D. C. Larbalestler, Nature (London) **364**, 129 (1993).
[4]A. Schilling, M. Cantoni, J. D. Guo, and H. R. Ott, Nature (London) **363**, 56 (1993).
[5]C. W. Chu, L. Gao, F. Chen, Z. J. Huang, R. L. Meng, and Y. Y. Xue, Nature (London) **363**, 323 (1993).
[6]U. Welp, G. W. Crabtree, J. L. Wagner, and D. C. Hinks, Physica C **218**, 373 (1993).
[7]C. P. Bean and J. D. Livingston, Phys. Rev. Lett. **12**, 14 (1964).
[8]P. G. de Gennes, *Superconductivity of Metals and Alloys* (Benjamin, New York, 1966), p. 79.
[9]L. Burlachkov, M. Konczykowski, Y. Yeshurun, and F. Holtzberg, J. Appl. Phys. **70**, 5759 (1991).
[10]S. T. Weir, W. J. Nellis, Y. Dalichaouch, B. W. Lee, M. B. Maple, J. Z. Liu, and R. N. Shelton, Phys. Rev. B **43**, 3034 (1991).
[11]N. Chikumoto, M. Konczykowski, N. Motohira, and A. P. Malozemoff, Phys. Rev. Lett. **69**, 1260 (1992).
[12]Ming Xu, D. K. Finnemore, G. W. Crabtree, V. M. Vinokur, B. Dabrowski, D. G. Hinks, and K. Zhang, Phys. Rev. B **48**, 10 630 (1993).
[13]J. R. Clem, in *Proceedings of the 13th Conference on Low Temperature Physics (LT13),* edited by K. D. Timmerhaus, W. J. O'Sullivan, and E. F. Hammel (Plenum, New York, 1974), Vol. 3, p. 102.
[14]L. Burlachkov, Phys. Rev. B **47**, 8056 (1993).
[15]M. Paranthaman, J. R. Thompson, Y. R. Sun, and J. Brynestad, Physica C **213**, 271 (1993).
[16]H. Zijlstra, *Experimental Methods in Magnetism* (North-Holland, Amsterdam, 1967).
[17]M. Konczykowski, L. I. Burlachkov, Y. Yeshurun, and F. Holtzberg, Phys. Rev. B **43**, 13 707 (1991).
[18]J. R. Thompson, J. G. Ossandon, D. K. Christen, B. C. Chakoumakos, Y. R. Sun, M. Paranthaman, and J. Brynestad, Phys. Rev. B **48**, 14 031 (1993).
[19]V. G. Kogan, M. M. Fang, and Sreeparna Mitra, Phys. Rev. B **38**, 11 958 (1988).
[20]V. G. Kogan, M. Ledvij, A. Yu. Simonov, J. H. Cho, and D. C. Johnston, Phys. Rev. Lett. **70**, 1870 (1993).
[21]J. R. Clem, J. Appl. Phys. **50(5)**, 3518 (1979).
[22]H. R. Kerchner, J. O. Thomson, and R. Feenstra, in *Advances in Cryogenic Engineering: Materials,* edited by F. R. Fickett and R. P. Reed (Plenum, New York, 1992), Vol. 38B, p. 997.
[23]A. M. Campbell, J. Phys. C **2**, 1492 (1969).
[24]J. A. Lewis, C. E. Platt, M. Wegmann, M. Teepe, J. L. Wagner, and D. G. Hinks, Phys. Rev. B **48**, 7739 (1993).
[25]J. Schwartz, S. Nakamae, G. W. Raben, Jr., J. K. Heuer, S. Wu, J. L. Wagner, and D. G. Hinks, Phys. Rev. B **48**, 9932 (1993).
[26]M. R. Beasley, R. Labusch, and W. W. Webb, Phys. Rev. B **181**, 682 (1969).